ELSEVIER

www.elsevier.nl/locate/jorganchem

Journal of Organometallic Chemistry 611 (2000) 514–524

Journal of Organometallic Chemistry

Quantum chemical study of parasitic reaction in III–V nitride semiconductor crystal growth

Koichi Nakamura [a], Osamu Makino [b], Akitomo Tachibana [a,*], Koh Matsumoto [c]

[a] *Department of Engineering Physics and Mechanics, Kyoto University, Kyoto 606-8501, Japan*
[b] *Department of Molecular Engineering, Kyoto University, Kyoto 606-8501, Japan*
[c] *NIPPON SANSO Corporation Tsukuba Laboratory, Tsukuba 300-2611, Japan*

Received 29 February 2000; accepted 26 March 2000

Abstract

We have discussed the gas-phase parasitic reactions in $M(CH_3)_3/H_2/NH_3$ systems following the elimination of methane by carrying out ab initio quantum chemical calculations, where M denotes Al, Ga, or In. It is clearly shown that the Al source gases enhance reactivity, and the adduct-derived chain compounds grow successively with high exothermicity. We have concluded that the strong Al–N coordination interaction contributes remarkably to the stabilization of the reaction system. In the presence of excess ammonia, we have proved that potential energy barrier of the methane elimination is reduced considerably. The methane elimination by reaction of carrier H_2 gas with $M(CH_3)_3$ is also exothermic.

Keywords: Parasitic reactions; Gas-phase reaction; Nitride semiconductor; Quantum chemical calculation; Regional density functional theory

1. Introduction

Wide-band-gap GaN and related nitrides have attracted much attention because of their application for blue light-emitting diodes and lasers [1,2]. Rapid progress in the metal–organic vapor phase epitaxy (MOVPE) technology makes it possible to fabricate highly efficient GaN and InGaN devices in atmospheric pressure [1–8].

However, the epitaxial growth of devise-quality III–V nitrides is further complicated by the severe interaction of precursors in gas phase. Particularly in the case of AlGaN alloys in atmospheric-pressure MOVPE, in contrast to GaN and InGaN, the growth of AlGaN layers is inhibited by gas-phase reactions among precursors leading to adduct formation, called 'parasitic reactions' [3–5]. Recently, Matsumoto et al. suppressed convection using a three-layered laminar flow reactor and succeeded to reduce parasitic reactions among trimethylaluminum (TMA), trimethylgallium (TMG), and ammonia [3]. This shows that the advanced control and knowledge of gas-phase reaction is very important, but it is difficult to resolve gas-phase reaction mechanism by observation especially in atmospheric pressure.

For high-temperature gas-phase reactions between TMG and ammonia, Thon and Kuech studied the reaction mechanism by means of in situ mass spectroscopy in an isothermal flow tube reactor for $TMG/H_2/ND_3$ system [4]. They clarified that the main gas-phase species is $[(CH_3)_2GaNH_2]_x$ resulting from the very fast adduct formation by elimination of a methane molecule, which is observed only as a form of CH_3D. On the contrary, no CH_3D molecule is observed in $TMG/D_2/NH_3$ system. They concluded that all gas-phase elimination of methane results from an intramolecular reaction of $TMG{\cdot}NH_3$ complex or between the adduct-derived species and the excess ammonia. However, it is presumed that the CH_3D molecule could be also detected through other intermolecular reactions between two of the ammonia complexes, between the precursor and the complex, between the adduct-derived compounds, and so on.

In $TMA/H_2/NH_3$ and $TMG/H_2/NH_3$ systems, several theoretical studies for diffusion of system based on the simulations by means of the reactor model have been performed [9,10].We have reported the detailed reaction

* Corresponding author. Tel.: +81-75-7535184; fax: +81-75-7535184.
E-mail address: akitomo@scl.kyoto-u.ac.jp (A. Tachibana).

0022-328X/00/$ - see front matter
PII: S0022-328X(00)00403-4

mechanism of the parasitic reactions between TMA, TMG, and ammonia by quantum chemical approach [11–13]. In this paper, we have investigated many sorts of the gas-phase reactions in $M(CH_3)_3/H_2/NH_3$ systems following the elimination of methane, above all in the presence of excess ammonia, where M denotes Al, Ga, or In for TMA, TMG, or trimethylindium (TMI) respectively, by carrying out ab initio quantum chemical calculations. We shall elucidate the detailed energetics and the possible reaction mechanisms of the parasitic processes and verify that the epitaxial growth rate of AlGaN device abruptly starts to drop in atmospheric-pressure MOVPE.

2. Computational methods and basis sets

Ab initio quantum chemical calculations were performed with the GAUSSIAN-94 program package [14]. The geometries of model reaction species and transition states (TSs) for the methane elimination were optimized by the analytical energy gradient method at the Lee–Yang–Parr gradient-corrected correlation functional [15] with the Becke's three hybrid parameters (B3LYP) [16], using double zeta basis set with the Hay–Wadt's effective core potential (ECP) [17,18] on the metal atoms and the Dunning–Huzinaga's full double-zeta gaussian basis set [19] on the other atoms, called LanL2DZ basis set. Except for hydrogen atom, the Huzinaga's polarization functions [20] were added to the basis set (LanL2DZ*). The Mulliken population analysis was carried out by means of the Kohn–Sham (KS) orbitals [21]. The bond order B_{AB} between atom A and atom B is given by [22–25]:$B_{AB} = \Sigma_{\mu\in A}\Sigma_{\nu\in B}(\mathbf{PS})_{\mu\nu}(\mathbf{PS})_{\nu\mu}$where **P** is the density matrix and **S** is the overlap matrix, respectively.

3. Results and discussion

3.1. Electronic process in coordination interaction

$M(CH_3)_3$ molecule (**1**; each one respectively denotes **1a**, **1g**, and **1i** for M = Al, Ga, and In, and so forth) makes a very stable complex with ammonia, $(CH_3)_3M{\cdot}NH_3$ (**2**), due to the M–N coordinate bond as you know:

$$M(CH_3)_3\ (\mathbf{1}) + NH_3 \rightarrow (CH_3)_3M{\cdot}NH_3\ (\mathbf{2}) \quad (1)$$

On the other hand, TMA monomers are known to form stable $Al_2(CH_3)_6$ dimers which have a four-membered ring stabilized by intermolecular Al–C interaction [26,27], as follows:

$$2Al(CH_3)_3\ (\mathbf{1a}) \rightarrow [Al(CH_3)_3]_2 \quad (2)$$

in contrast to TMG and TMI. Certainly, the stabilization energy for dimerization of two of monomer **1** is -10.15, -0.07, and -1.45 kcal mol^{-1} for TMA, TMG, and TMI, respectively, per one dimer formation, in our calculation at the B3LYP/LanL2DZ* level. In the dimer form, the Al–C bonds are lengthened by ca. 0.19 Å as compared with those of the monomer, and therefore it is expected easily that the weak Al–C bond in dimer would accept a part in the high reactivity of methane elimination by ammonia. However, we confirmed that TMA dimer dissociates immediately to two monomers as an ammonia molecule approaches, and then one of them makes the complex **2a**:

$$[Al(CH_3)_3]_2 + NH_3 \rightarrow Al(CH_3)_3\ (\mathbf{1a}) + (CH_3)_3Al{\cdot}NH_3\ (\mathbf{2a}) \quad (3)$$

Fig. 1 is a molecular orbital (MO) energy correlation diagram for the formation of the complex **2** from **1** and ammonia at the RHF/LanL2DZ* level. It means that the NH_3 lone pair HOMO and $M(CH_3)_3$ MOs including HOMO and LUMO fabricate hybrid orbitals and that the $(CH_3)_3M{\cdot}NH_3$ system gains large stabilization energy. According to this interaction explained by using MOs, charge transfer occurs from NH_3 to **1**. As shown in Table 1, both of the stabilization energy of complex formation and the M–N bond order is the largest in the TMA + NH_3 system, but the quantities of charge transfer from ammonia to TMA and to TMG are almost equal to each other in terms of the Mulliken population analysis. We found that each of TMA monomer, the $Al(CH_3)_3$ part and the NH_3 part in complex **2a** is polarized more remarkably than the corresponding TMG monomer and parts in complex **2g**, from the results of atomic charges as listed in Table 1. Therefore it is considered that the difference in the M–N bonding energies between **2a** and **2g** is caused by the dipole–dipole interaction between **1** and ammonia. In the TMI + NH_3 system, the largest polarization of the same kind is observed, but the stabilization energy of complex formation is small because the charge transfer from ammonia to TMI is poor.

Here, we shall investigate the electronic processes of the formation of coordinate bond between **1** and ammonia in terms of the regional density functional theory [28–34]. Fig. 2(a) shows electron acceptor region *P* in the box and an electron donor region *Q* which we set up. The regional electron number of the region, N_P, was computed by means of the analytical integration algorithm [34]. As shown in Fig. 2(b), change of N_P along the reaction coordinate indicates that charge transfer acceptabilities of TMA and TMG are almost equal, and that of TMI is inferior to others.

3.2. Elimination of methane by unimolecular mechanism

As mentioned in introduction, Thon and Kuech reported that the elimination of a single CH_3D molecule by an immediate reaction between TMG and ND_3 occurs in $TMG/H_2/ND_3$ system [4]. We have investigated the reaction mechanism of the methane elimination by the intramolecular reaction of the complexes **2**, called unimolecular mechanism:

$$M(CH_3)_3\ (\mathbf{1}) + NH_3 \rightarrow (CH_3)_3M{\cdot}NH_3\ (\mathbf{2})$$

$$(CH_3)_3M{\cdot}NH_3\ (\mathbf{2}) \rightarrow [\mathbf{TS1}]^{\ddagger} \rightarrow M(CH_3)_2NH_2\ (\mathbf{3}) + CH_4 \quad (4a)$$

$$n\,M(CH_3)_2NH_2\ (\mathbf{3}) \rightarrow [M(CH_3)_2NH_2]_n \quad (4b)$$

As shown in Table 2, the elimination of methane (reaction 4a) is an exothermic reaction, leading to an amide compound, $M(CH_3)_2NH_2$ (**3**). Fig. 3 and Table 3 show optimized structure and the geometrical parameters of **TS1**, respectively. The amide adduct **3** is strikingly stabilized by dimerization, trimerization, and more, leading to $[M(CH_3)_2NH_2]_n$ (reaction 4b) with a ring form or a chain form, as shown in Table 4. As discussed below, **3** also makes stable complex with **1** or ammonia, without potential energy barrier. Note that the activation energy of **TS1a** is about half of the others, **TS1g** and **TS1i**. Judging from bond orders in **TS1**, it is considered that the difference in the activation energies would be caused by each strength of the M–N interaction. Fig. 4 shows the 17th KS orbitals of **TS1** which are respectively concerned with the progress of the CH_4 elimination most dominantly in each system. The thickness of in-phase lobe along N···H···C is largest, and simultaneously, lobe of N also spreads out toward M most extensively in the $TMA + NH_3$ system. This appearance implies that the M–N interaction in **TS1** is certainly most strong in the $TMA + NH_3$ system, and the difference in the strength of the M–N interaction would affect the activation energy as same as the formation energy of the complex **2**.

3.3. Elimination of methane by bimolecular mechanism

Furthermore, we have discussed intermolecular reactions in $M(CH_3)_3/H_2/NH_3$ system. Due to the collision of species, intermolecular reactions bring about the energy transfer from transition energies of each species to the internal energy of reaction system, and the

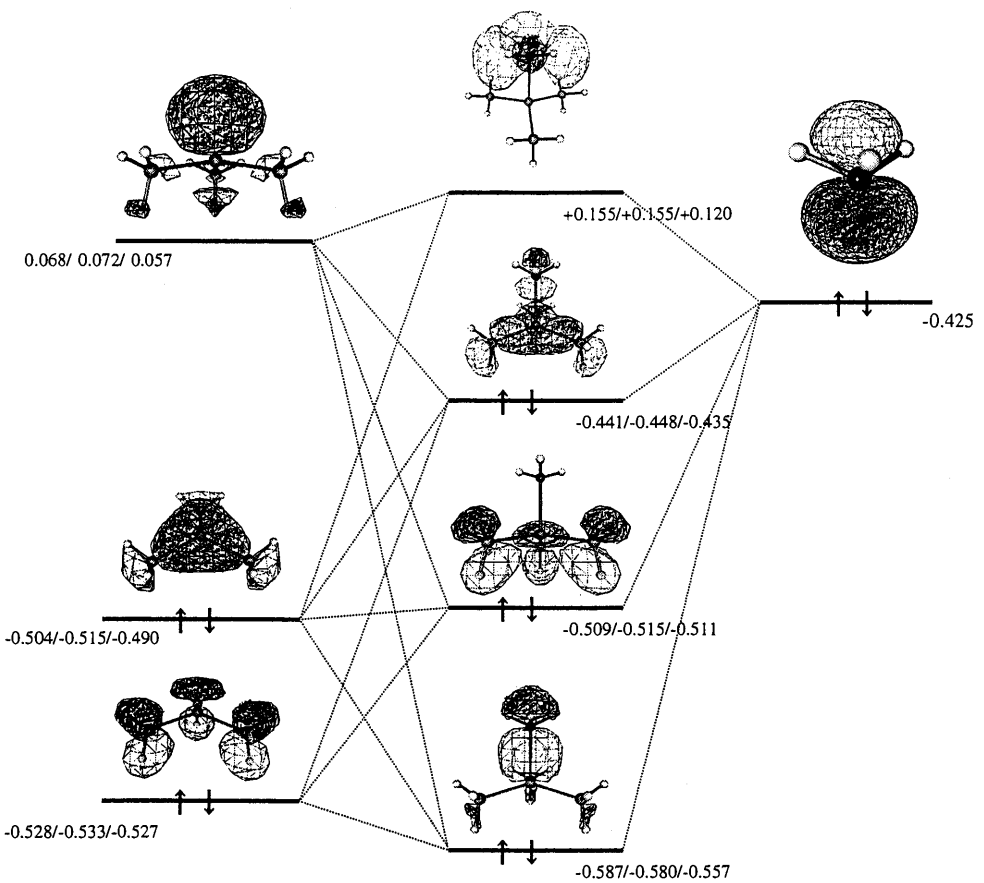

Fig. 1. Molecular orbital energy correlation diagram for the formation of the complex $(CH_3)_3M{\cdot}NH_3$ (**2**) from TMA/TMG/TMI (**1**) and NH_3. Attached orbital energies are in the units of eV, at the RHF/LanL2DZ* level.

Table 1
Stabilization energy (kcal mol^{-1}) and Mulliken population analysis of $(CH_3)_3M{\cdot}NH_3$ complex formation

	M		
	Al	Ga	In
Stabilization energy (kcal mol^{-1})	−23.17	−18.92	−18.22
Bond order of M–N in **2**	0.337	0.287	0.194
Mulliken charge transfer for $NH_3 \Rightarrow$ **1** in **2**	0.179	0.179	0.128
Atomic charge in ***1***			
M	0.962	0.869	1.054
C	−1.024	−1.006	−1.084
Axial-H	0.233	0.238	0.243
Equatorial-H	0.235	0.239	0.245
(CH_3 part)	(−0.321)	(−0.290)	(−0.352)
Atomic charge in NH_3			
N	−0.898	−0.898	−0.898
H	0.299	0.299	0.299
Atomic charge in ***2***			
M	1.008	0.878	1.112
C	−1.048	−1.017	−1.103
Axial-H	0.230	0.234	0.238
Equatorial-H	0.211	0.216	0.225
(CH_3 part)	(−0.396)	(−0.352)	(−0.414)
N	−0.943	−0.925	−0.966
Amino-H	0.374	0.368	0.365

Table 2
Relative energies (kcal mol^{-1}) of CH_4 elimination by unimolecular mechanism in $M(CH_3)_3$–NH_3 system with results of population analysis for $(CH_3)_3M{\cdot}NH_3$ complex

	M		
	Al	Ga	In
1 + NH_3	0	0	0
2	−23.17	−18.92	−18.22
TS1	7.37	14.83	13.96
3 + CH_4	−27.02	−22.62	−19.09

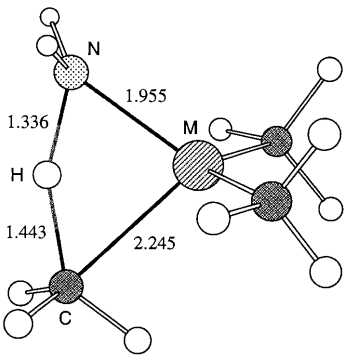

TS1

Fig. 3. B3LYP/LanL2DZ* optimized structure of **TS1** with M = Al (**TS1a**). All bond lengths are in Å.

reaction often becomes easy to proceed. Here, we shall discuss the reaction mechanism of the methane elimination between the complex **2** and another $M'(CH_3)_3$ molecule (**1′**), called bimolecular mechanism:

$$M(CH_3)_3\ (\mathbf{1}) + NH_3 \rightarrow (CH_3)_3M{\cdot}NH_3\ (\mathbf{2})$$

$$(CH_3)_3M{\cdot}NH_3\ (\mathbf{2}) + M'(CH_3)_3\ (\mathbf{1'}) \rightarrow [\mathbf{TS2}]^{\ddagger} \rightarrow (CH_3)_3M{\cdot}NH_2M'(CH_3)_2\ (\mathbf{4}) + CH_4 \quad (5a)$$

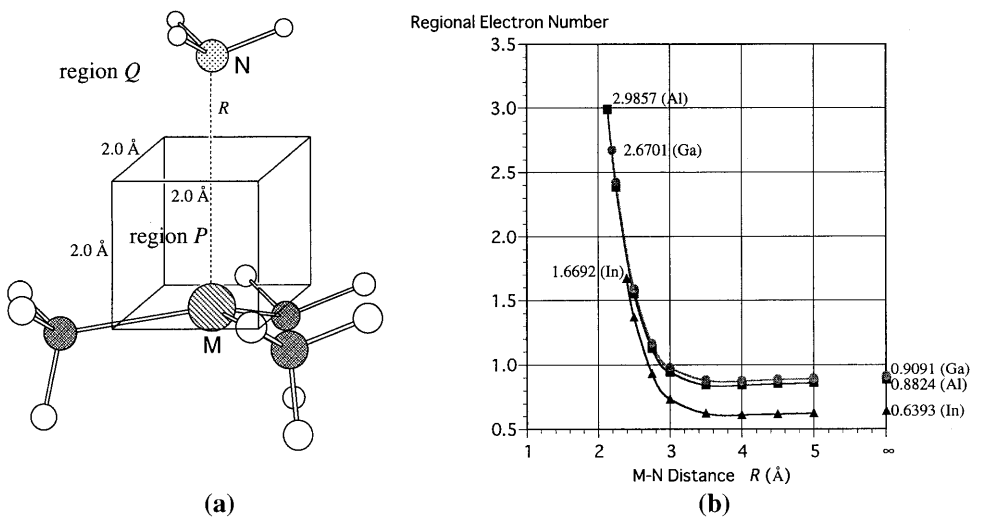

(a) **(b)**

Fig. 2. (a) Regional partitioning and (b) regional electron number N_P in $\mathbf{1} + NH_3$ system. *P* and *Q* denote an electron acceptor region and an electron donor region, respectively.

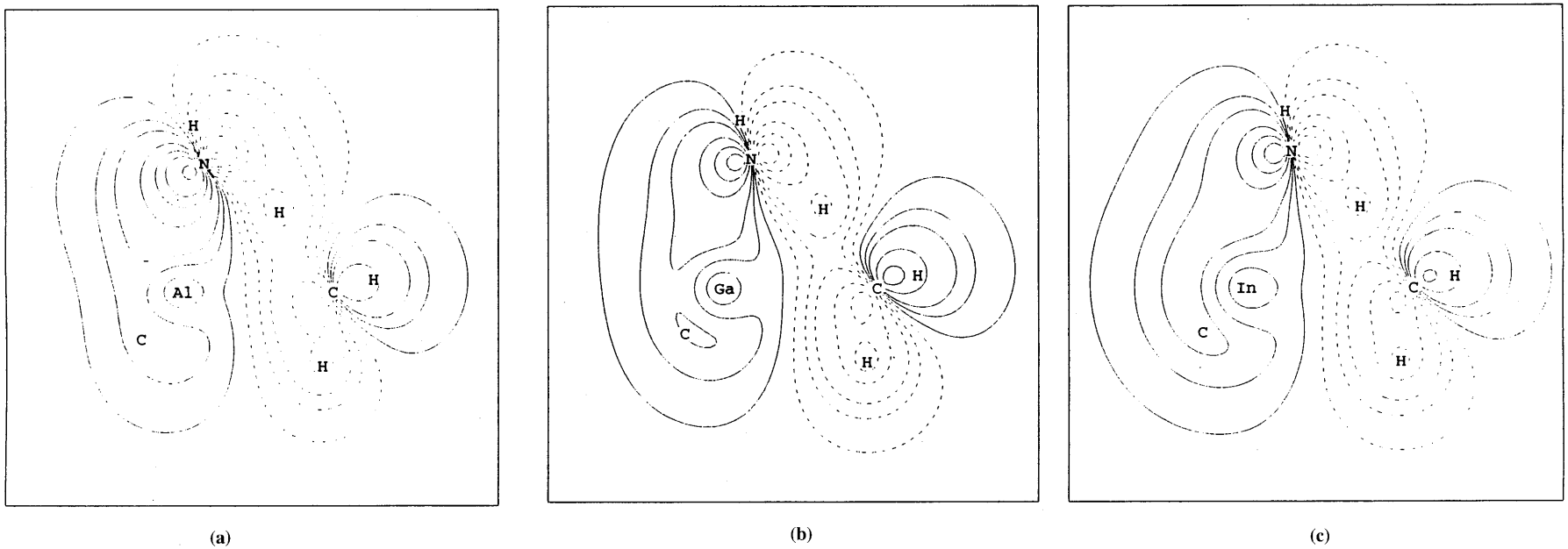

Fig. 4. Contour maps of 17th KS orbital of **TS1** in a mirror plane of C_s symmetry, containing metal, nitrogen, and eliminating carbon: (a) **TS1a**, (b) **TS1g**, and (c) **TS1i**. Solid lines denote positive values and dashed lines denote negative values.

$$(CH_3)_3M{\cdot}NH_2M'(CH_3)_2\ (\mathbf{4}) + NH_3 \rightarrow (CH_3)_3M{\cdot}NH_2M'(CH_3)_2{\cdot}NH_3\ (\mathbf{5}) \quad (5b)$$

Table 3
Bond lengths (Å) and bond orders [a] in **TS1**

M	M–N	N–H	H–C	C–M
Al	1.955 (0.649)	1.336 (0.314)	1.443 (0.408)	2.245 (0.448)
Ga	1.993 (0.603)	1.331 (0.317)	1.440 (0.410)	2.307 (0.416)
In	2.165 (0.492)	1.326 (0.333)	1.445 (0.433)	2.500 (0.349)

[a] Values in parenthesis.

Table 4
Dimerization and trimerization energies of amide adduct $M(CH_3)_2NH_2$ (kcal mol^{-1})

	M		
	Al	Ga	In
Ring form			
$2M(CH_3)_2NH_2 \rightarrow [M(CH_3)_2NH_2]_2$	−51.96	−44.91	−49.85
$3M(CH_3)_2NH_2 \rightarrow [M(CH_3)_2NH_2]_3$	−82.43	−71.13	−77.38
Chain form			
$2M(CH_3)_2NH_2 \rightarrow [M(CH_3)_2NH_2]_2$	−13.44	−10.23	−14.33
$3M(CH_3)_2NH_2 \rightarrow [M(CH_3)_2NH_2]_3$	−52.22	−38.39	−33.44

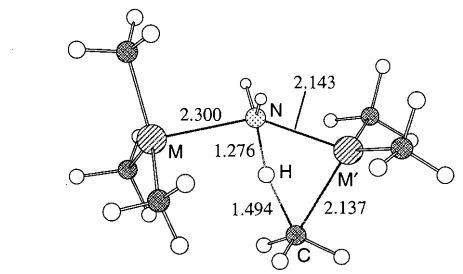

(a) **TS2**

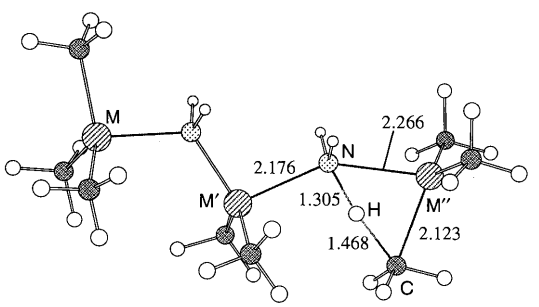

(b) **TS3**

Fig. 5. B3LYP/LanL2DZ* optimized structures of (a) **TS2** with M = M′ = Al and (b) **TS3** with M = M′ = M″ = Al.

$$(CH_3)_3M{\cdot}NH_2M'(CH_3)_2{\cdot}NH_3\ (\mathbf{5}) + M''(CH_3)_3\ (\mathbf{1''}) \rightarrow [\mathbf{TS3}]^{\ddagger} \rightarrow (CH_3)_3M{\cdot}NH_2M'(CH_3)_2{\cdot}NH_2M''(CH_3)_2\ (\mathbf{6}) + CH_4 \quad (5c)$$

where M′ and M″ denote Al, Ga, or In, similarly as M. Fig. 5 and Table 5 respectively show optimized structures and the geometrical parameters of **TS2** and **TS3**. In reaction 5a, the eliminating methane molecule consists of a methyl group in **1′** and a hydrogen atom attached to nitrogen in the complex **2**. As shown in Fig. 5(a) and the upper half of Table 5, geometry of **TS2** in a $NH_3M'(CH_3)_3$ part is quite similar to that of **TS1**. The activation energies of **TS2** are reduced as compared with those of **TS1**, as it can be verified by comparing Table 2 with Table 6. It is considered that the additional interaction between $M(CH_3)_3$ and NH_3 as well as the regular M′–N interaction of **TS1** in the unimolecular mechanism stabilizes the system. This explanation is supported by an observation that activation energies are remarkably reduced when M = Al, which makes a stronger M–N orbital interaction.

After the elimination of a methane molecule, the remainder of the products make a four-membered ring compound or a MNM′ chain compound $(CH_3)_3M{\cdot}NH_2M'(CH_3)_2$ (**4**). These compounds correspond to the complexes of the amide adduct **3′** with **1**, as mentioned in the previous section. In particular, the chain compound makes a stable complex with NH_3, $(CH_3)_3M{\cdot}NH_2M'(CH_3)_2{\cdot}NH_3$ (**5**), again by a strong M′–N orbital interaction (reaction 5b), and the elimination of a methane molecule by bimolecular mechanism with another $M''(CH_3)_3$ molecule (**1″**) would take place, leading to a MNM′NM″ compound **6** (reaction 5c). As shown in Fig. 5(b) and the lower half of Table 5, geometry of **TS3** in a M′–$NH_3M''(CH_3)_3$ part is also quite similar to that of **TS2** in a M–$NH_3M'(CH_3)_3$ part. The activation energies of **TS3** are remarkably close to those of corresponding **TS2** if one notes that M′ and M″ in **TS3** respectively correspond to M and M′ in **TS2**, as listed in Table 6. It means that the kind of M in **TS3** hardly depends on the activation energy. Therefore, it is clarified that the activation energy of the bimolecular mechanism is dominated only by two of the M–N orbital interactions in the local part where the elimination of a methane molecule occurs, even if the chain compound is lengthened. Similarly as **4**, the chain form of **6** makes a stable complex with NH_3 again, and the MNMNMN… chain grows succeedingly with high exothermicity.

TMG and TMI are somewhat hard to react with the chain compound as compared with TMA, above all when Ga–N–Ga, Ga–N–In, and In–N–In bonds are fabricated. On the contrary, the energetics of the bimolecular mechanism is reduced considerably when the system

Table 5
Bond lengths in **TS2** and **TS3** (Å)

TS2	M	M′		M′–N	N–H	H–C	C–M′	M–N
	Al	Al		2.143	1.276	1.494	2.137	2.300
	Ga	Al		2.026	1.294	1.479	2.183	2.719
	Al	Ga		2.253	1.315	1.456	2.176	2.204
	Ga	Ga		2.104	1.292	1.473	2.214	2.577
	In	Ga		2.100	1.291	1.471	2.220	2.738
	Ga	In		2.280	1.289	1.480	2.409	2.593
	In	In		2.279	1.286	1.479	2.413	2.749
TS3	M	M′	M″	M″–N	N–H	H–C	C–M″	M′–N
	Al	Al	Al	2.266	1.305	1.468	2.123	2.176
	Ga	Al	Al	2.254	1.302	1.470	2.124	2.184
	Al	Ga	Al	2.065	1.276	1.492	2.167	2.662
	Ga	Ga	Al	2.043	1.283	1.486	2.178	2.758
	Al	Al	Ga	2.362	1.346	1.433	2.169	2.133
	Ga	Al	Ga	2.349	1.342	1.435	2.169	2.141
	Al	Ga	Ga	2.300	1.324	1.446	2.177	2.248
	Ga	Ga	Ga	2.284	1.319	1.450	2.178	2.263
	In	Ga	Ga	2.306	1.323	1.447	2.173	2.223
	Ga	In	Ga	2.194	1.286	1.470	2.196	2.578
	In	In	Ga	2.194	1.286	1.470	2.196	2.567
	Ga	Ga	In	2.517	1.324	1.447	2.368	2.219
	In	Ga	In	2.513	1.323	1.447	2.368	2.218
	Ga	In	In	2.439	1.293	1.467	2.380	2.483
	In	In	In	2.438	1.292	1.467	2.380	2.480

Table 6
Relative energies of CH_4 elimination by bimolecular mechanism for the first and second steps (kcal mol^{-1})

First step [a]	M	M′		**1**+**1**′+NH_3	**2**+**1**′	**TS2**	**4**+CH_4
	Al	Al		0	−23.17	2.97	−45.09
	Ga	Al		0	−18.92	4.85	−40.65
	Al	Ga		0	−23.17	8.40	−41.91
	Ga	Ga		0	−18.92	11.54	−37.41
	In	Ga		0	−18.22	10.90	−36.78
	Ga	In		0	−18.92	10.78	−37.91
	In	In		0	−18.22	10.04	−36.69
Second step [b]	M	M′	M″	**4**+**1**′+NH_3	**5**+**1**′	**TS3**	**6**+CH_4
	Al	Al	Al	0	−23.53	3.18	−45.50
	Ga	Al	Al	0	−23.15	3.57	−45.10
	Al	Ga	Al	0	−19.72	6.12	−41.37
	Ga	Ga	Al	0	−19.32	6.18	−44.78
	Al	Al	Ga	0	−23.53	7.73	−42.83
	Ga	Al	Ga	0	−23.15	8.17	−42.29
	Al	Ga	Ga	0	−19.72	11.39	−41.87
	Ga	Ga	Ga	0	−19.32	11.78	−37.97
	In	Ga	Ga	0	−19.36	6.14	−38.08
	Ga	In	Ga	0	−18.79	11.33	−37.23
	In	In	Ga	0	−18.98	11.12	−37.45
	Ga	Ga	In	0	−19.32	10.29	−38.93
	In	Ga	In	0	−19.36	10.29	−39.03
	Ga	In	In	0	−18.79	10.05	−37.56
	In	In	In	0	−18.98	9.81	−37.77

[a] Reactions 1 and 5a.
[b] Reactions 5b and 5c.

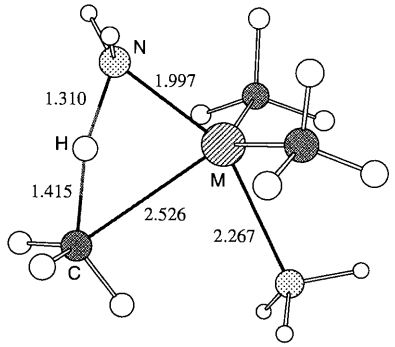

TS4

Fig. 6. B3LYP/LanL2DZ* optimized structure of **TS4** with M = Al. All bond lengths are in Ångstroms.

contains Al more plentifully. It indicates that the parasitic reaction is sensitive to quantity of Al. Due to the successive reactions of (A) complex formation with ammonia and (B) elimination of methane by the bimolecular mechanism, the chain structure of AlGaN aggregates would be propagated with low potential energy barrier.

3.4. Effect of excess ammonia

In this section, we discuss the reaction mechanism of **1** in the presence of excess ammonia. Under this condition, **1** makes a stable complex due to the coordination bond with two ammonia molecules, $H_3N{\cdot}(CH_3)_3M{\cdot}NH_3$ (**7**), without potential energy barrier as follows:

$$M(CH_3)_3\ (\mathbf{1}) + NH_3 \rightarrow (CH_3)_3M{\cdot}NH_3\ (\mathbf{2})$$

$$(CH_3)_3M{\cdot}NH_3\ (\mathbf{2}) + NH_3 \rightarrow H_3N{\cdot}M(CH_3)_3{\cdot}NH_3\ (\mathbf{7}) \quad (6)$$

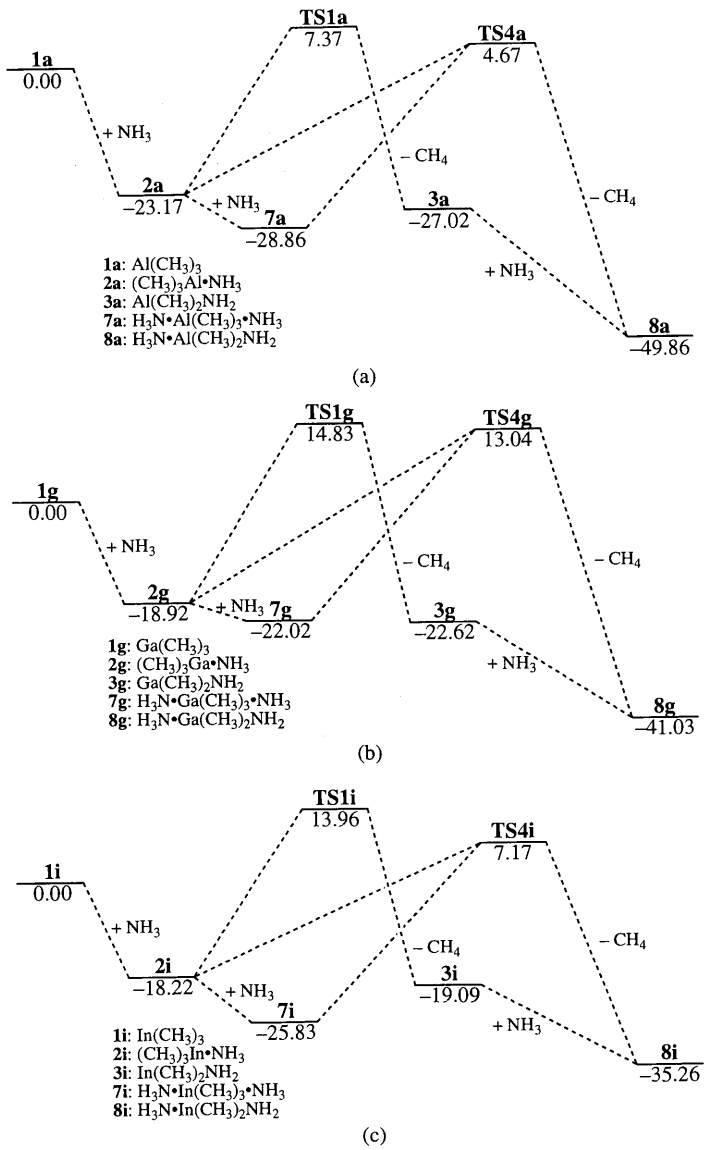

Fig. 7. Potential energy diagram for the elimination of methane in (a) TMA/NH_3, (b) TMG/NH_3, and (c) TMI/NH_3 system for the unimolecular mechanism at the B3LYP/LanL2DZ* level. All results are in kcal mol^{-1}.

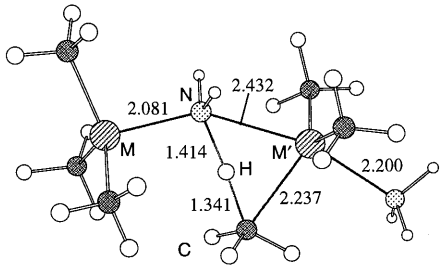

TS5

Fig. 8. B3LYP/LanL2DZ* optimized structure of **TS5** with M = M′ = Al. All bond lengths are in Ångstroms.

Table 7
Relative energies of CH_4 elimination by unimolecular mechanism from amide adduct $M(CH_3)_2NH_2$ and NH_3 (kcal mol^{-1})

	M		
	Al	Ga	In
3 + $2NH_3$	0	0	0
8 + NH_3	−22.84	−18.41	−16.17
TS6 + NH_3	13.41	18.02	19.05
9 + CH_4 + NH_3	−23.10	−18.37	13.96
TS7	3.11	13.03	7.20
10 + CH_4	−47.56	−38.34	−31.24

Table 8
Relative energies of CH_4 elimination by reaction between $M(CH_3)_3$ and carrier H_2 gas (kcal mol^{-1})

	M		
	Al	Ga	In
1 + H_2	0	0	0
$(CH_3)_3M{\cdot}H_2$	−0.55	−0.43	−0.54
TS8	28.91	33.96	35.41
$M(CH_3)_2H + CH_4$	−9.28	−10.65	−11.93

The elimination of a methane molecule can take place in the presence of excess ammonia, by an intramolecular reaction of the complex **7** or an intermolecular collision between the complex **1** and an ammonia molecule:

$$H_3N{\cdot}M(CH_3)_3{\cdot}NH_3\ (\mathbf{7})\ [\text{or}\ (CH_3)_3M{\cdot}NH_3\ (\mathbf{2}) + NH_3] \rightarrow [\mathbf{TS4}]^{\ddagger} \rightarrow H_3N{\cdot}M(CH_3)_2NH_2\ (\mathbf{8}) + CH_4 \quad (7)$$

As shown in Fig. 6, geometry of **TS4** in the local part where the elimination of a methane molecule occurs is quite similar to that of **TS1**. The product **8** corresponds to a complex of the amide adduct **3** in reaction 4a with an ammonia. Fig. 7 shows the potential energy diagram in the $M(CH_3)_3/NH_3$ system for the unimolecular mechanism, which is redefined as a mechanism of the methane elimination from one $M(CH_3)_3$ precursor-derived species, where the relative energies are standardized by setting the energy of the $M(CH_3)_3 + 2NH_3$ system to zero. It is found that potential energy barrier is reduced through **TS4** in the presence of excess ammonia for each of $\mathbf{1} + 2NH_3$ system. In particular, potential energy barrier for TMA is reduced to 4.67 kcal mol^{-1}. Accordingly, it is considered that the gas-phase reaction of TMA proceeds rapidly in the presence of excess ammonia. Since the stabilization energy of the coordination by a second ammonia molecule (reaction 4) is relatively small, the main stream of reaction 5 would be the intermolecular reaction between the complex **2** and an ammonia molecule with the effective energy transfer due to the collision.

The elimination of a methane molecule by the bimolecular mechanism in the previous section does not occur in the presence of excess ammonia because **1**′, **1**″,..., respectively, have formed a complex with ammonia immediately. Therefore, we shall discuss here the intermolecular reaction between two complexes **2** and **2**′ as follows:

$$(CH_3)_3M{\cdot}NH_3\ (\mathbf{2}) + (CH_3)_3M'(CH_3)_3\ (\mathbf{2}') \rightarrow [\mathbf{TS5}]^{\ddagger} \rightarrow (CH_3)_3M{\cdot}NH_2M'(CH_3)_2{\cdot}NH_3\ (\mathbf{5}) + CH_4 \quad (8)$$

Optimized geometry of **TS5** is shown in Fig. 8. The product of reaction 8 is identical with the complex obtained in reaction 5b. Fig. 9 shows the potential energy diagram in the $M(CH_3)_3/NH_3$ system for the bimolecular mechanism, which is redefined as a mechanism of the methane elimination from two $M(CH_3)_3$ precursor-derived species, where the relative energies are standardized by setting the energy of the $M(CH_3)_3 + M'(CH_3)_3 + 2NH_3$ system to zero. Relative energies of **TS5** in the presence of excess ammonia are lower than those of **TS2**. Accordingly, the parasitic reaction should proceed rapidly in the presence of excess ammonia.

Furthermore, we have discussed the unimolecular mechanism between the amide adduct **3** and excess ammonia:

$$M(CH_3)_2NH_2\ (\mathbf{3}) + NH_3 \rightarrow H_3N{\cdot}M(CH_3)_2NH_2\ (\mathbf{8}) \quad (9)$$

$$H_3N{\cdot}M(CH_3)_2NH_2\ (\mathbf{8}) \rightarrow [\mathbf{TS6}]^{\ddagger} \rightarrow MCH_3(NH_2)_2\ (\mathbf{9}) + CH_4 \quad (10)$$

$$H_3N{\cdot}M(CH_3)_2NH_2\ (\mathbf{8}) + NH_3 \rightarrow [\mathbf{TS7}]^{\ddagger} \rightarrow H_3N{\cdot}MCH_3(NH_2)_2\ (\mathbf{10}) + CH_4 \quad (11)$$

Relative energies for each state are listed in Table 7. As compared with Fig. 7, potential energy barriers are relatively higher than corresponding barriers of the $M(CH_3)_3/NH_3$ system, but the elimination of methane can occur in particular for M = Al.

3.5. Reactions with carrier hydrogen gas

According to Thon and Kuech, none of hydrogen atoms of eliminating methane originates from carrier H_2

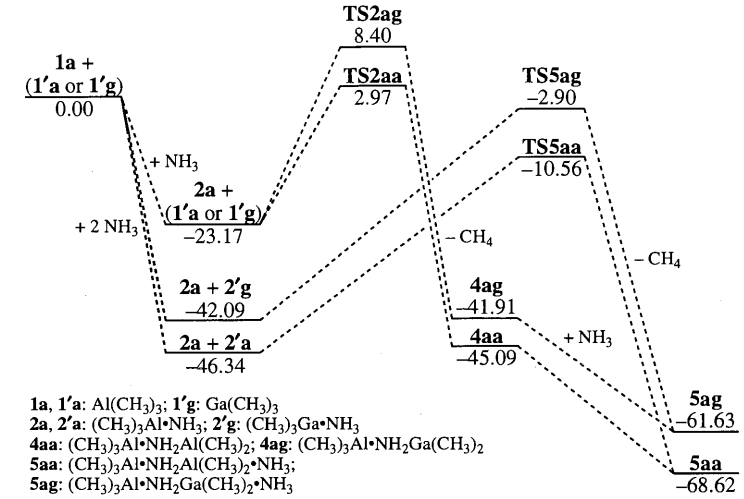

(a)

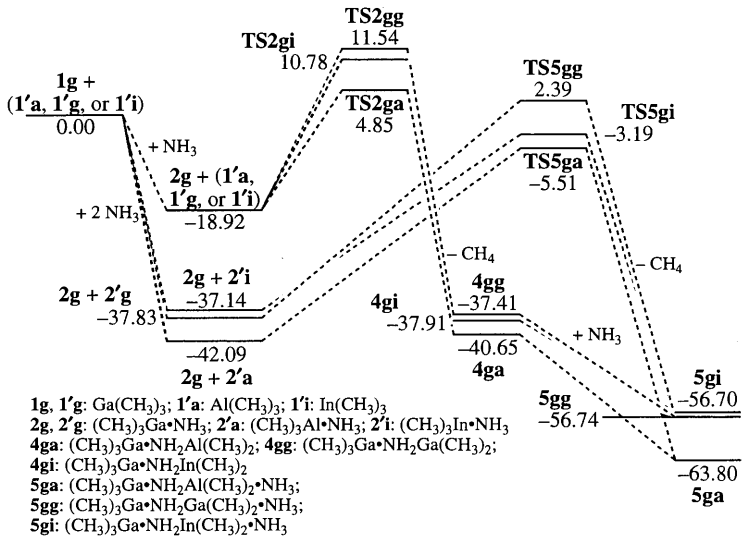

(b)

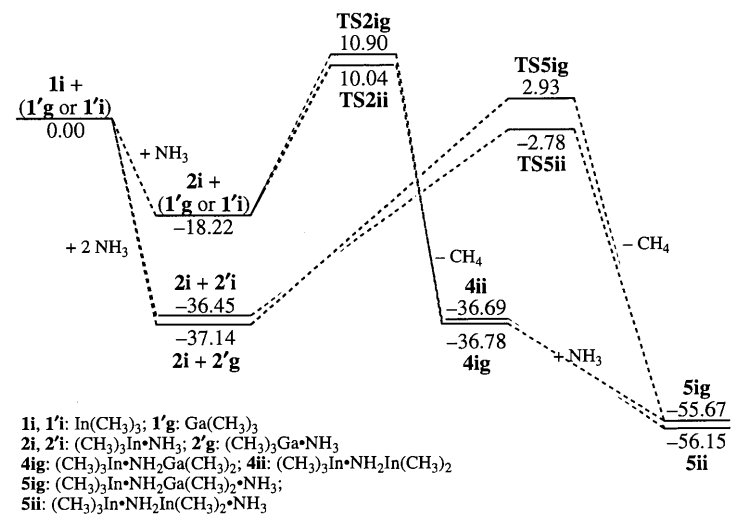

(c)

Fig. 9. Potential energy diagram for the elimination of methane in $M(CH_3)_3/M'(CH_3)_3/NH_3$ system for the bimolecular mechanism with M = (a) Al, (b) Ga, and (c) In at the B3LYP/LanL2DZ* level. All results are in kcal mol^{-1}.

gas in $TMG/H_2/NH_3$ system [4]. We have discussed here reaction between **1** and H_2 gas leading to the elimination of a methane molecule,

$$M(CH_3)_3\ (\mathbf{1}) + H_2 \rightarrow [\mathbf{TS8}]^{\ddagger} \rightarrow M(CH_3)_2H + CH_4 \qquad (12)$$

As shown in Table 8, reaction 12 is exothermic for each $\mathbf{1} + H_2$ system, and activation energy is not quite high as compared with other chemical reactions in general. However, reactivity of H_2 gas is extremely reduced in $M(CH_3)_3/H_2/NH_3$ system. We found the $(CH_3)_3M{\cdot}H_2$ complex, where the distance between M and the closer atom of H_2 is so long as 2.926, 3.027, and 3.127 Å for TMA, TMG, and TMI, respectively. The stabilization energy is infinitesimal because H_2 molecule has no lone pair and therefore cannot make a coordinate bond with **1**. Therefore, H_2 in the complex should be rapidly affected by substitution of an ammonia molecule in $M(CH_3)_3/H_2/NH_3$ system, and then H_2 gas cannot approach to **1**. Judging from potential energy barrier in reaction 12, it is considered that the elimination of a methane molecule can take place due to reaction 12 in the absence of ammonia. In fact, it is indicated that CH_4 molecule is produced at temperatures < 500°C in TMG/H_2 system [4].

4. Conclusions

We have discussed the gas-phase parasitic reactions in $M(CH_3)_3/H_2/NH_3$ systems following the elimination of methane. It is clearly shown that the Al source gases enhance reactivity, and the adduct-derived chain compounds grow successively with high exothermicity. We have demonstrated that the strong Al–N coordination interaction contributes remarkably to the stabilization of the reaction system, by means of the detailed analysis of the electronic process and the reaction mechanism. Therefore, the fine control of the Al–N coordination interaction would make possible it to control the parasitic reactions; for example, the substitution of metal source may have a possibility of inhibiting the parasitic reactions, discussed in our previous paper [13]. In the presence of excess ammonia, we have proved that potential energy barrier of the methane elimination is further reduced. The methane elimination by reaction of carrier H_2 gas with $M(CH_3)_3$ is exothermic, and it is probably able to proceed in the absence of ammonia.

Acknowledgements

This work was supported by a grant-in-aid for Scientific Research from the Ministry of Education, Science and Culture of Japan, for which the authors express their gratitude. Authors wish to thank the Computer Center of Institute for Molecular Science and Data Processing Center of Kyoto University, for their generous permission to use the HITAC M-680 and S-820, and FACOM M-780/30, VP-400E, and VP-200 computers, respectively.

References

[1] S. Nakamura, Acta Phys. Pol. Sect. A 95 (1999) 153 and references therein.
[2] I. Akasaki, H. Amano, Jpn. J. Appl. Phys. 36 (1997) 5393 and references therein.
[3] K. Uchida, H. Tokunaga, Y. Inashi, N. Akutsu, K. Matsumoto, Mater. Res. Soc. Symp. Proc. 449 (1997) 129.
[4] A. Thon, T.F. Kuech, Appl. Phys. Lett. 69 (1996) 55.
[5] C.H. Chen, H. Liu, D. Steigerwald, W. Imler, C.P. Kuo, M. Ludowise, S. Lester, J. Amano, J. Electron Mater. 25 (1996) 1004.
[6] J.P. Noad, A.J. SpringThorpe, J. Electron Mater. 9 (1980) 601.
[7] S.J. Bass, C. Pickering, M.L. Young, J. Crystallogr. Growth 64 (1983) 68.
[8] C.P. Kuo, J.S. Yuan, R.M. Cohen, J. Dunn, G.B. Stringfellow, Appl. Phys. Lett. 44 (1984) 550.
[9] T.G. Mihopoulos, V. Gupta, K.F. Jensen, J. Crystallogr. Growth 195 (1998) 733.
[10] S.A. Safvi, J.M. Redwing, M.A. Tischer, T.F. Kuech, J. Electrochem. Soc. 144 (1997) 1789.
[11] A. Tachibana, K. Nakamura, O. Makino, H. Tokunaga, N. Akutsu, K. Matsumoto, Second Proceedings of the second International Symposium on Blue Laser and Light Emitting Diodes, 1998, p. 308, Tu-P5 (late news).
[12] A. Tachibana, O. Makino, S. Tanimura, H. Tokunaga, N. Akutsu, K. Matsumoto, Phys. Stat. Sol. Sect. A 176 (1999) 699.
[13] O. Makino, K. Nakamura, A. Tachibana, H. Tokunaga, N. Akutsu, K. Matsumoto, Appl. Surf. Sci. 159–160 (2000) 374.
[14] M.J. Frisch, G.W. Trucks, H.B. Schlegel, W.P.M. Gill, B.G. Johnson, M.A. Robb, J.R. Cheeseman, T.A. Keith, G.A. Patterson, J.A. Montgomery, K. Reghavachari, M.A. Al-Laham, V.G. Zakrzewski, J.V. Ortiz, J.B. Foresman, J. Cioslowski, B.B. Stefanov, A. Nanayakkara, M. Challacombe, C.Y. Peng, P.Y. Ayala, W. Chen, M.W. Wong, J.L. Andres, E.S. Replogle, R. Gomperts, R.L. Martin, D.J. Fox, J.S. Binkley, D.J. Defrees, J. Baker, J.J.P. Stewart, M. Head-Gordon, C. Gonzalez, J.A. Pople, GAUSSIAN-94, Gaussian Inc., Pittsburgh PA, 1995.
[15] C. Lee, W. Yang, R.G. Parr, Phys. Rev. Sect. B 37 (1988) 785.
[16] A.D. Becke, J. Chem. Phys. 98 (1993) 5648.
[17] P.J. Hay, W.R. Wadt, J. Chem. Phys. 82 (1985) 270.
[18] P.J. Hay, W.R. Wadt, J. Chem. Phys. 82 (1985) 299.
[19] T.H. Dunning Jr., P.J. Hay, in: H.F. Schaefer III (Ed.), Modern Theoretical Chemistry, Plenum, New York, 1976.
[20] S. Huzinaga et al. (Eds.), Gaussian basis sets for molecular calculations, Elsevier, New York, 1984, p. 23.
[21] W. Kohn, L.J. Sham, Phys. Rev. Sect. A 140 (1965) 1133.
[22] I. Mayer, Chem. Phys. Lett. 97 (1983) 270.
[23] I. Mayer, Theor. Chim. Acta 67 (1985) 315.
[24] I. Mayer, Int. J. Quant. Chem. 29 (1986) 73.
[25] I. Mayer, Int. J. Quant. Chem. 29 (1986) 477.
[26] C.H. Henrickson, D.P. Eyman, Inorg. Chem. 6 (1967) 1461.
[27] A.W. Laubengayer, W.F. Gilliam, J. Am. Chem. Soc. 63 (1941) 477.
[28] A. Tachibana, Int. J. Quant. Chem. Symp. 21 (1987) 181.
[29] A. Tachibana, R.G. Parr, Int. J. Quant. Chem. 41 (1992) 527.
[30] A. Tachibana, Int. J. Quant. Chem. 57 (1996) 423.
[31] A. Tachibana, Theor. Chem. Acc. 102 (1999) 188.
[32] A. Tachibana, K. Nakamura, J. Am. Chem. Soc. 117 (1995) 3605.
[33] A. Tachibana, S. Kawauchi, K. Nakamura, H. Inaba, Int. J. Quant. Chem. 57 (1996) 673.
[34] A. Tachibana, K. Nakamura, K. Sakata, T. Morisaki, Int. J. Quant. Chem. 74 (1999) 669.